International Journal of Innovative Technology and Exploring Engineering (IJITEE)
ISSN: 2278-3075 (Online), Volume-9 Issue-2, December 2019

Modeling the Heating in a High Temperature Superconducting Current Carrying Element in Fault Current Limiters

Alexander S. Maklalov, Vladimir I. Scherbakov, Daria A. Gorbunova

Abstract*: Mathematical model was developed for modeling the increase temperature in high temperature superconducting (HTS) current carrying element in superconducting fault current limiters (SFCL). The variation in the heating up of HTS element along its length is a result primarily of the variation in its resistance that has to do with the manufacturing process employed to make it.The model was developed and mathematical modeling of the process was carried out in the Comsol MultiPhysics software package. Element that was tested was a 12 mm wide stack of three stainless steel tapes and three HTS soldered to each other. In order to get more precise parameters for the models the cross-sectional thermal conductivity was measured for the stacks of HTS of two different types. The estimates obtained using the model were very close to experimental data. The impact was also studied of the spread of the electrical resistance of HTS on how fast the current carrying element made from it heated up.

Keywords* : HTS elements, Mathematical model, S-innovation, Suman, Temperature variations, Thermal conductivity.

I. INTRODUCTION

Using of the superconducting fault current limiters (SFCL) in networks allows drastic decrease of fault currents, enhancing the reliability of the power system and reduce the wear of electrical equipment [1-5]. Currently, efforts aimed at creating SFCL are underway around the world [6-10], with several dozen systems having been developed and currently undergoing trials [11-17]. The operation of resistive-type SFCL is based on the physical properties of a superconductor: if the current is less than a critical value, the device has zero resistance and has no impact on the operation of the circuit **Error! Reference source not found.**. In the event of a short circuit, the current exceeds the threshold value causing the SFCL to transition to a resistive state, thus limiting the current to the nominal value [19].

Revised Manuscript Received on December 30, 2019.
***** Correspondence Author
Alexander S. Maklalov, S-Innovations LLC, Moscow, Russia. Email: a.**maklakov**@superox.ru
Vladimir I. Scherbakov*, S-Innovations LLC, Moscow, Russia. Email: v.scherbakov74@mail.ru
Daria A. Gorbunova, S-Innovations LLC, Moscow, Russia. Email: d.gorbunova@superox.ru

As a result of the short circuit current being limited, a large amount of heat is generated in high temperature superconducting (HTS) element, which can have an adverse effect on its properties or even cause it to disintegrate [20-23]. Because of this situation it was felt that there was a need for a mathematical model that would make it possible to estimate the increase in the temperature of HTS element [24].
It should be noted that HTS element may heat up unevenly both along the length and across the cross-section [25]. The variation in the heating up of HTS element along its length is a result primarily of the variation in its resistance that has to do with the manufacturing process employed to make it.
The variation in how the HTS element heats up across the cross-section stems from its structure that is comprised of a large number of layers of various types of materials many of which have anisotropic properties [26-28]. The situation is complicated further when instead of a single high temperature superconducting tape, a stack of soldered tapes is used because the thermal conductivity of the soldered joints is determined to a large extent by the soldering process used and can thus only be determined experimentally.

II. EXPERIMENTAL PART

A. Inputs

The properties and characteristics of the materials used in this study are presented in Table 1.

Table 1: Information about the high temperature superconducting tapes used in the study

Manufacturer	S-innovation	Suman
Substrate material	Hastelloy alloy C-276	Stainless steel AISI 310
Substrate thickness, *um*	100	100
Resistance per unit of length at room temperature, *mOhm/m*	175	187
Resistance per unit of length at the liquid nitrogen boiling temperature, *mOhm/m*	39	42
Thickness of the silver layer (face/back), *um*	2/1	2/1
Thickness of the copper layer (face/back), *um*	1.5/1.5	1/1

B. Measuring the transverse thermal conductivity of high temperature superconducting tape stacks

In order to measure the transverse thermal conductivity of high temperature superconducting tapes manufactured by S-Innovation (Russia) and Sunam (South Korea), two samples were prepared, each a stack of 100 soldered layers (see Fig. 1). The HTS tapes were coated in a layer of silver 1 um thick, on top of each a layer of copper 1.5-2 um thick was added.

HTS tapes were subjected to hot tinning to apply a coat of 6 um thick PSAg solder. After being hot tinned the HTS tapes were cut up into squares with 12 um long sides, gathered into stacks and soldered to each other in a press at a temperature of +200°C. During the soldering process the stacks were pressed together with a force of 2 kN.

Rose's alloy was used to solder copper plates onto both sides of each stack of HTS tapes with a blind hole being drilled in the sides of the plates to install Pt 100 temperature sensors. Rose's alloy was used to solder a silicon diode on top of one of the copper plates; this was later used as the heater.

The process used for measuring the transverse thermal conductivity of a stack of HTS tapes is depicted on Fig. 1. A heat conducting adhesive was used to glue the sample to the bottom of a stainless steel double-walled mug on the inside of the mug. The wires from the temperature sensors and the heater were run outside through a hermetically sealed connector. A vacuum pump was used to pump air out of the space between the walls of the mug to reduce the pressure down to 10 3 mbar.

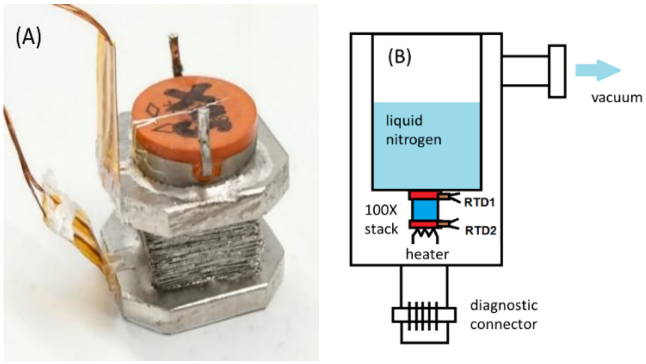

Fig. 1. A diagram of a sample and the set-up used to measure the thermal conductivity of a stack of HTS tapes.

Liquid nitrogen was poured into the mug to measure thermal conductivity at a temperature of 77 K. The mug was empty when the thermal conductivity was measured at room temperature. By changing the current running through the diode it is easy to estimate how the amperage affects the temperature of the sample and from that a thermal conductivity coefficient can be estimated. The measurement results are depicted in Fig. 2.

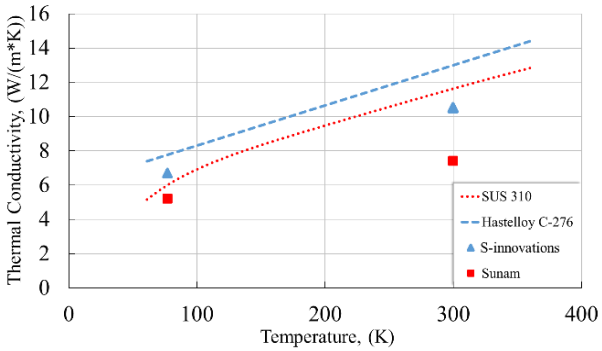

Fig. 2. The thermal conductivity of AISI 310 stainless steel and Hastelloy alloy C-276 (reference data), the transverse thermal conductivity values for stacks of HTS tapes manufactured by S-innovations and Sunam at 77 K and 300 K

It was demonstrated that the thermal conductivity of a stack of HTS tapes is very close to the thermal conductivity of their base material: Hastelloy for S-Innovation tapes and stainless steel for the Sunam tapes. The correlations between the temperature and thermal conductivity for the base materials were taken from literature [29, 30]. The thermal conductivity values of the buffer and HTS ceramic layers don't have much impact on the transverse thermal conductivity of the stack. The differences in the thermal conductivity of HTS tape stacks and their base material are probably owing to the thermal conductivity of the soldered joints. Sunam HTS tapes have a distinctive sickle shape, which negatively impacts the thermal conductivity of their soldered joints compared to S-Innovations HTS tapes.

C. Measuring the heating up of sample HTS tape stacks with current impulse

We studied HTS elements in the form of soldered stacks of three HTS tapes and three stainless steel tapes (90 um thick AISI 304 steel). A 1.5-2 um thick layer of copper was applied to 12 mm thick HTS tapes already covered in a 1 um layer of silver. After HTS tapes were covered a 6-um thick layer of PSAg solder. Total thickness of HTS tapes were a 115 um. The stacks were soldered in a press, stainless steel and HTS tapes were alternated in each stack. Massive copper contacts were soldered to the ends of the sample stacks. A total of two samples were assembled in this manner: one made using HTS tapes made by S-Innovation and the other from HTS tapes made by Sunam. Each sample was 76 cm long (with a 50 cm long working area).

In order to use a current impulse to measure the heating up of HTS element samples, a test circuit was assembled on the basis of a powerful step-down transformer (see Fig. 3). Switch S1 was used to switch the primary coil in order to set the voltage in the secondary coil to 10, 13 or 16 V (the effective values), which correspond to voltage drops in the sample of 20, 26 or 32 V/m.

Switch K1 is closed to simulate a short circuit. The current flowing through the sample is a function of the active and reactive resistance of the connection buses, the sample being used and the transformer coils, seeing how these values are sufficiently small, the surge current may be as high as 6 kA or more.

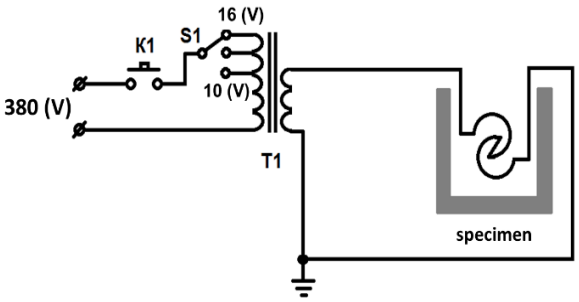

Fig. 3. The test circuit.

The time it takes switch K1 to actuate is set by the digital time relay with an accuracy of 10 ms. The current in the sample is measured using a current transformer. The voltage current in the sample are recorded digitally using a multi-channel gauge. The change in the resistance of the samples over time is estimated using discrete mathematics methods based on the values of the current and voltage with subsequent smoothing out of the curve to suppress the 50 Hz pulses.

The temperatures of the HTS current carrying elements are determined from their resistance. The samples were affixed to a massive aluminium frame that was cooled down to the required temperature by doses of liquid nitrogen, while the resistance of the samples was measured in 4 points. For convenience's sake the dependencies of resistance on temperature were normalized to the resistance at room temperature (see Fig. 4).

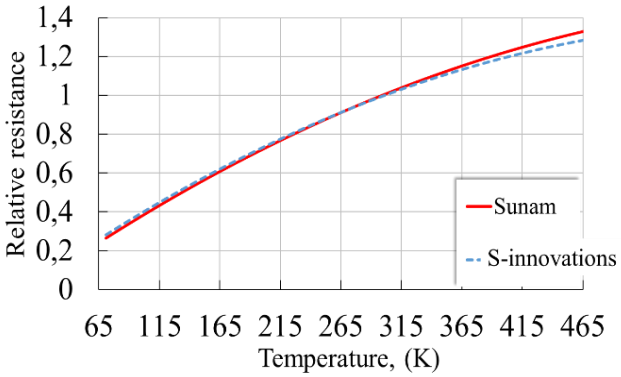

Fig. 4. The normalized dependencies of the resistance of HTS current carrying elements on temperature.

III. RESULTS AND DISCUSSION

A. Modeling

The heating of samples was modeled in the Comsol MultiPhysics software package using the finite element method in 2D geometry. This was done using the Heat Transfer in Solids software package.

The experimentally determined changes over time of the voltage on the sample and the current flowing through it were used to estimate the amount of heat generated in the sample during the test. To that end the dependencies of the effective voltage and current on time were estimated using the floating window algorithm with the values being averaged over one full period of voltage at the industrial frequency, i.e. over 20 ms.

Because a HTS tape comprises multiple layers of materials with the thickness of adjacent layers often varying by several orders of magnitude, modeling this type of material requires a lot of time and significant amounts of computing power. For this reason, we simplified our mathematical model in a number of ways. The samples were represented as 2D objects and all calculations were carried out across the cross section of the samples (Fig. 5).

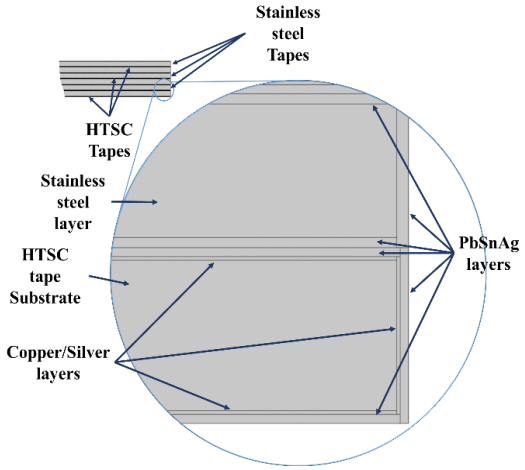

Fig. 1. 2D geometry was used to model the samples.

In addition, based on the experimental data for the thermal conductivity of the HTS tapes (Fig. 2) under consideration that we obtained earlier and the fact that only small amounts of heat get generated when the short circuit currents flow through the buffer layers and the HTS layer due to a high electric resistance, we decided to not include those layers in the model. Since silver and copper are substances with very similar electric and heat properties and seeing how there is no clear cut boundary between the silver and copper layers in the HTS tapes due to the mutual diffusion of the two substances, our model uses a single copper/silver layer. The geometric models of tape samples from the two manufacturers different in the thickness of some layers. In addition, the models used different substrate materials in the HTS tapes (Table 2).

Table 2: Samples modeling parameters

Parameter	S-innovation sample	Suman sample
HTS tape base material	Hastelloy alloy C-276	Stainless steel AISI 310
The HTS tape substrate material thickness, *um*	100	100
The HTS tape substrate material width, *mm*	12	12
The thickness of the silver/copper layer on the side of the HTS tape, *um*	2	2.5
The thickness of the solder layer on the side of the HTS tape, *um*	6	6
The thickness of the solder on the side of the stainless steel tape, *um*	6.7	6.7
The thickness of the solder layer on the side of the stainless steel tape, *um*	8	8.5
The width of the AISI 304 stainless steel tape, *mm*	12	12
The thickness of the AISI 304 stainless steel tape, *um*	88.9	88.9

When the sample limits short circuit current, heat is generated in it, which is then dissipated across the layers that the sample is made up of. In order to correctly model the distribution of temperature across a sample, weight coefficients were introduced into the model; these were calculated for each layer as follows:

$$P = K_s(T)*P+K_{Cu}(T)*P+K_{PbSnAg}(T)*P+K_{AISI304}(T)*P, \quad (1)$$

Where P is the heat power generated in the sample; $K_s(T)$, $K_{Cu}(T)$, $K_{PbSnAg}(T)$ $K_{AISI304}(T)$ are the weight coefficient for the HTS tape base material, copper, solder and AISI 304 stainless steel respectively.

$$K_s(T) = \frac{1}{R_s^{-1}(T)+(R_{Cu}^{-1}(T)+R_{PbSnAg}^{-1}(T)+R_{AISI304}^{-1}(T))*R_s(T)}, \quad (2)$$

Where $R_s(T)$, $R_{cu}(T)$, $R_{PbSnAg}(T)$, $R_{AISI304}(T)$ are the values of resistance per meter of sample length of the HTS tape base material, copper, solder and AISI 304 stainless steel, respectively.

During the production of HTS tapes and further manufacture of samples from them the actual thickness of the metal layers can differ from the target value. As a result, the thickness of each layer can very over length and that can have an effect on the local resistance of the tapes, the heat generated in specific points when the tapes are being used to limit short circuit currents and the temperature gradient in the samples. In order to take this factor into account in the model, we've introduced a 1.2% variation in resistance at room temperature along the length of the HTS tape and a 15% variation in the resistance of the solder at room temperature along the length of the tape. Thus, two extreme cases were modeled: one with thin layers of solder and copper/silver and one with thick layers of solder and copper/silver.

$$P = K_R*P_{av}, \quad (3)$$

Where P is the amount of heat generated in the sample with the variation in layer thickness taken into account, Pav is the amount of heat generated in the sample as estimated based on experimental data KR is the coefficient determining the change in the resistance of the entire sample as a result of change in the resistance of the individual tapes it is comprised of.

$$K_R = \frac{R_{ss}^{-1}+R_{HTS}^{-1}}{R_{ss}^{-1}+K_{RHTS}^{-1}*R_{HTS}^{-1}}, \quad (4)$$

Where R_{ss} is the resistance of the three AISI 304 stainless steel tapes that are part of the sample including the resistance of the solder in them; R_{HTS} is the resistance of all the HTS tapes, including the solder in them. R_{ss} and R_{HTS} are calculated as parallel circuit resistances. K_{RHTS} is the coefficient defining the difference between the HTS tape resistance in the solder and the average HTS tape resistance (in this model it is assumed to be equal to 0.925 for the thinnest possible thicknesses of the solder and copper/silver layers and 1.075 for the maximum thicknesses of the solder and copper/silver layers). The resistance of one HTS tape with a finishing copper coating can be calculated using the formula:

$$R_{HTS} = ((R_S)^{-1}+(R_{Cu})^{-1})^{-1}, \quad (5)$$

In order to account for variation in the thickness of the copper/silver layer, we've introduced the K_{RHTSCu} coefficient into the model, setting it to 1.006 for the thin copper/silver layer and to 0.994 for the thick layer:

$$K_{RHTSCu}*R_{HTSCu} = ((R_S)^{-1}+(K_{RCu}*R_{Cu})^{-1})^{-1}, \quad (6)$$

This formula was used to estimate coefficient K_{RCu} reflecting how much the copper resistance in the HTS tape changes when the overall resistance of the tape increases or decreases by 0.6%.

$$R_{HTSPbSnAg} = ((R_s)^{-1}+(R_{Cu})^{-1}+(R_{PbSnAg})^{-1})^{-1}, \quad (7)$$

In this manner the coefficient $R_{HTSPbSnAg}$ was introduced to reflect the impact of variation in the thickness of the solder layer, which was set to 1.075 for the thin solder layer case and to 0.925 for the thick solder layer case.

$$K_{RHTSPbSnAg} * R_{HTSPbSnAg} = \frac{1}{R_S^{-1}+R_S^{-1}+K_{RPbSnAg}^{-1}*R_{PbSnAg}^{-1}}, \quad (8)$$

This was then used to estimate the coefficient $K_{RPbSnAg}$ which reflects how much the solder resistance in the HTS tape changes when the total resistance of the tape increases or decreases by 7.5% The two modeled samples had the following values for these coefficients in **Error! Reference source not found.**

Table 3: Values of the coefficients for modeling

Parameter	S-innovation sample	Suman sample
The value K_{RCu} for a thick layer of copper	0.992	0.992
The value K_{RCu} for a thin layer of copper	1.008	1.008
The value $K_{RPbSnAg}$ for a thick layer of solder	0.769	0.714
The value $K_{RPbSnAg}$ For a thin layer of solder	1.231	1.286

Since the electrical resistance of a conductor changes in reverse proportion to the area of its cross section, the coefficients we calculated show the factor by which the total cross-sectional area of the copper and solder layers changes in the stack when the resistance of an HTS tape with a finishing copper layer changes by 1.2% and that of an HTS tape with a finishing solder layer changes by 15%. These coefficients were then used to estimate the coefficients $K_s(T)$, $K_{Cu}(T)$, $K_{PbSnAg}(T)$ $K_{AISI304}(T)$ (for thin and thick layers of copper/silver and solder).

Throughout the experiment the sample was kept in liquid nitrogen. When the sample is limiting short circuit current, some of the heat generated in it is used up to vaporize liquid nitrogen. After the HTS sample transition from superconductivity to normal conductivity, all the nitrogen around the sample evaporates.

The sample that ends up in a gas cushion and for a period of 25 ms there is practically no dissipation of heat into the nitrogen: the process flows adiabatically. This is followed by a quasi-equilibrium mode in which the gas moves up away from the sample and is replaced by liquid nitrogen that continues to boil and evaporate. The dissipation of heat into liquid nitrogen occurring in this manner is very well studied in literature.

The existing studies allowed us to estimate the dependence between the heat dissipated into the liquid nitrogen and the temperature of the sample.

In our model we used the formula found in [28] to describe this process mathematically. The dependency was introduced into the model as a condition applicable to the external boundaries of the sample and represents negative power: a function of the temperature of the sample generated along its boundaries.

In order to take into account, the primary adiabatic process that produces the gas cushion [31-34], the function was also multiplied a piecewise function over time whose value equals zero up to 25 ms and then 1 after 25 ms [35-37].

B. Findings

In our calculations we used the Time Dependent Study for an interval of time between zero and 350 ms. Calculations were carried out for six cases: for the minimal and maximum thicknesses of silver/copper and solder layers and for three cases used in the experiment with voltages per unit of length of 20 V/m, 26 V/m and 32 V/m.

Once calculations were completed graphs were constructed showing the dependencies of temperature on time and these were compared with experimental data (Fig. 6, Fig. 8).

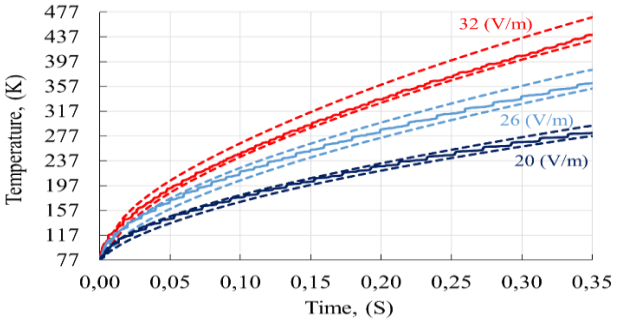

Fig. 6. The dependencies of temperature on time in a short circuit in four modes for the S-innovations sample (the red continuous lines) The estimated dependencies of the minimal (the blue dotted lines) and maximum (the blue continuous lines) temperatures in the stack on time.

The graphs showing the dependence between the average temperature across the volume of the stack on time in short circuits lasting 350 ms for the S-innovations sample (Fig. 6) suggest that the sample is in the safe interval of temperatures (below than the melting temperature for the PSAg solder) if the voltage drop in it is 20 V/m and 26 V/m.

The graph showing the experimental results for a voltage of 32 V/m contains a deflection point that corresponds to a solder melting point (Fig. 7).

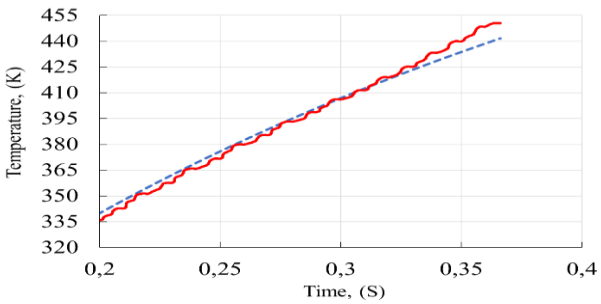

Fig. 7. The solder melting temperature gradient

At the deflection point the sample temperature averaged across its volume is 422 K. The melting temperature for PSAg solder is 453 K plus-minus 30 K.

The modeling of the heating up of a S-innovations sample confirms that there is only limited variation in the temperature across the volume of the stack.

According to the model, the temperature variation at the deflection point is 35 K.

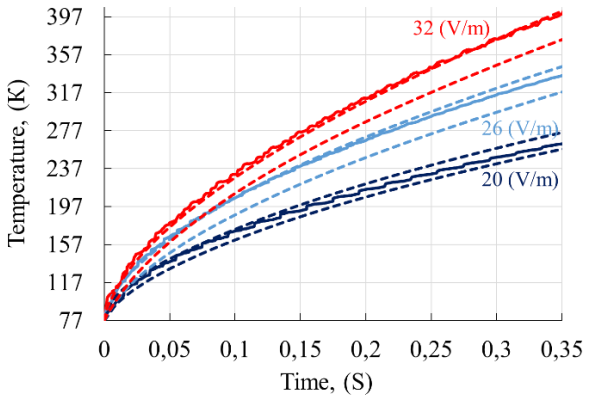

Fig. 8. The graphs showing the change in temperature over time in a short circuit for the four modes of the Sunam sample (the red continuous lines). The estimated dependencies of the minimal (the blue dotted lines) and maximum (the blue continuous lines) temperatures in the stack on time.

No solder melting temperature was observed in the Sunam sample (Fig. 8). Since the solder does not melt at the average sample volume temperature of 402 K, the variation of temperatures in this sample does not exceed 50 K.

IV. CONCLUSION

The modeling results bear out this conclusion. The difference between the minimal and maximum temperature in the model does not exceed 50 K. The HTS tapes from the two manufactures that were considered have thermal conductivity close to that of their base materials (buffer layers, as well as the superconducting layer do not make a big contribution). Nevertheless, when short circuit currents are being limited, a relatively small variation in temperatures results in the sample, stemming primarily from the variation in the thickness of the stabilizing metal layers along the length of the sample. Since for an HTS current carrying element, temperature variation is a critical parameter, measures must be taken during the manufacture of such elements to ensure that the thickness of the stabilizing levels remains constant throughout the length of the element.

REFERENCES

1. J. X. Jin, Y. J. Tang, X. Y. Xiao, B. X. Du, Q. L. Wang, J. H. Wang, S. H. Wang, Y. F. Bi, J. G. Zhu, "HTS Power Devices and Systems: Principles, Characteristics, performance, and Efficiency", *IEEE Transactions on Applied Superconductivity*, *26*(7). 2016. DOI: 10.1109/TASC.2016.2602346
2. D. Sharma, S. Bhushan, "Basic Concepts of Superconducting Fault Current Limiter", *IEEE 1st International Conference on Power Electronics, Inteligent Control and Energy Systems (ICPEICES)*. 2017. DOI: 10.1109/ICPEICES.2016.7853069

3. L. Ye, A.M. Campbell, "Case study of HTS resistive superconducting fault current limiter in electrical distribution systems", *Elsevier, Electric Power Systems Research, 77*. 2007. pp. 534-539. DOI: 10.1016/j.epsr.2006.05.007
4. M. Sjostrom, R. Cherkaoui, B. Dutoit, "Enhancement of Power System Transient Stability Using Superconducting Fault Current Limiters", *IEEE Transactions on Applied Superconductivity, 9*(2). 1999. DOI: 10.1109/77.783547
5. L. Ye, L. Lin, K. Juengst, "Application Studies of Superconducting Fault Current Limiters in Electric Power Systems*", IEEE Transactions on Applied Superconductivity, 12*(1). 2002. DOI: 10.1109/TASC.2002.1018545
6. H. Naji, N. Harid, H. Griffiths, "Enhancement of DUBAL Network Operational Performance Using HTS-FCL", *IEEE International Conference on High Voltage Engineering and Application (ICHVE)*. 2018. DOI: 10.1109/ICHVE.2018.8642234
7. X. Xian-Yong, L. Yang, J. Jian-Xun, L. Chang-Song, X. Fang-Wei, "HTS Applied to Power System: Benefits and Potential Analysis for Energy Conservation and Emission Reduction", *IEEE Transactions on Applied Superconductivity, 26*(7). 2016. DOI: 10.1109/TASC.2016.2594800
8. L. Jiang, J. X. Jin, X. Y. Chen, "Fully Controled Hybrid Btidge Type Superconducting Fault Current Limiter*", IEEE Transactions on Applied Superconductivity, 24*(5). 2014. DOI: 10.1109/TASC.2014.2351264
9. E.M.W. Leung, G.W. Albert, M. Dew, P. Gurrola, K. Muehleman, B. Gamble, C. Russo, G. Dishaw, H. Boeing, D. Peterson, A. Rodrigues, "High temperature superconducting fault current limiter for utility applications", *Springer, Advances in Cryogenic Engineering Materials, 42*. 1996. pp. 961-968, 1996. DOI: 10.1007978-1-4757-9059-7_126
10. X. J. Jin, S. X. Dou, H. K. Liu, "Electrical Application of High Tc Superconducting Saturable Magnetic Core Fault Current Limiter", *IEEE Transactions On Applied Superconductivity, 7*(2). 1997.DOI: 10.1109/77.614678
11. Oksana. V. Savchina, Olga. V. Savchina, A. L. Bobkov, A. Z. Sharashidze, "On the State of the Mortgage Market in the Russian Federation in the Conditions of Global Economic Crisis", *Journal of Applied Economic Sciences, 11*(6(44)). 2016. pp. 39-41.
12. A. L. Tishchenko, V. S. Gorskii, N. S. Sergeeva, "Linear skin atrophy: Current information and modern approaches to the external therapy", *Medical News of North Caucasus, 13*(3). 2018. pp. 566-571. DOI: 10.14300/mnnc.2018.13106
13. J. Prigmore, N. Uzelac, "Fault Current Limiting (FCL) Devices and Techniques", in CIGRE Green Books (CIGREGB) (pp. 424-425). Cham: Springer, 2019.
14. J. Bock, M. Bludau, R. Dommerque, A. Hobl, S. Kraemer, M. O. Rikel, S. Elschner, "HTS Fault Current Limiters – First Commercial Devices for Distribution Level Grids in Europe*", IEEE Transactions on Applied Superconductivity, 21*(3). 2011. DOI: 10.1109/TASC.2010.2099636
15. Y. Xin, H. Hong, J. Z. Wang, W. Z. Gong, J. Y. Zhang, A. L. Ren, M. R. Zi, Z. Q. Xiong, D. J. Si, F. Ye, "Performance of the 35 kV/90 MVA SFCL in Live-Grid Fault Current Limiting Tests", *IEEE transactions on Applied Superconductivity, 21*(3). 2011. DOI: 10.1109/TASC.2011.2105452
16. M. Fotuhi-Firuzabad, D. Aminifar, I. Rahmati, "Reliability Study of HV Substations Equipped with the Fault Current Limiter", *IEEE Transactions on Power Delivery, 27*(2). 2012. DOI: 10.1109/TPWRD.2011.2179122
17. L. Xiao, L. Lin, "Recent Progress of Power Application of Superconductor in China*", IEEE Transactions on Applied Superconductivity, 17*(2). 2007. DOI: 10.1109/TASC.2007.898160
18. L. F. Martini, L. Bigoni, G. Cappai, R. Iorio, S. Malgarotti, "Analysis on the Impact of HTS Cables and Fault-Current Limiters on Power Systems", *IEEE Transactions on Applied Superconductivity, 13*(2). 2003. DOI: 10.1109/TASC.2003.812899
19. H. C. Freyhardt, "YBaCuO and REBaCuO HTS for Applications", *International Journal of Applied Ceramic Technology, 4*(3). 2007. DOI: 10.1111/j.1744-7402.2007.02134
20. F. Roy, B. Dutoit, F. Grilli, F. Sirois, "Magneto-Thermal Modeling of Second-Generation HTS for Resistive Fault Current Limiter Design Purposes", *IEEE Transactions on Applied Superconductivity, 18*(1). 2008. DOI: 10.1109/TASC.2008.917576
21. O. F. Putikov, N. P. Senchina, "Precise Solution of the System of Nonlinear Differential Equations in Partial Derivatives of the Theory of Geoelectrochemical Methods", *Doklady Akademii Nauk (Doklady Earth Sciences), 2*(463). 2015. pp. 726-727.
22. I. Telezhko, Yu. Biryukova, V. Kurilenko, "A model for forming tolerance in profession-oriented text translators as part of the process of developing their sociocultural competence", *Xlinguae, 12*(1). 2019. pp.116-124.
23. A. Tsvetkova, E. Katysheva, "Ecological and economic efficiency evaluation of sustainable use of mineral raw materials in modern conditions", *17th International Multidisciplinary Scientific Geoconference SGEM 2017. Conference Proceedings, 17*(53). pp. 241-247.
24. J.-Y. Yoon, S.-R. Lee, J.-Y. Kim, "R-type HTS EMTDC transient Model Considering Quenching and Recovery Characteristics", *Proceedings of the 5th WSEAS International Conference on Applications of Electrical Engineering, 5*(3). 2006. pp. 157-160.
25. B. Revaz, J. Y. Genoud, A. Junod, K. Neumaier, A. Erb, E. Walker, "d-Wave Scaling Relations in the Mixed-State Specific Heat of YBa2Cu3O7", *Physical Review Letters, 80*(15). 1998. DOI: 10.1103/PhysRevLett.80.3364
26. A. Junod, M. Roulin, B. Revaz, A. Mirmelstein,J.-Y. Genoud, E. Walker, A. Erb, "Specific Heat of High Temperature Superconductors in High Magnetic Fields", *Physica C: Superconductivity, 282-287*. 1997. pp. 1399-1400. DOI: 10.1016/S0921-4534(97)00794-6
27. A. Strizhenok, D. Korelskiy, "Assessment of the anthropogenic impact in the area of tailings storage of the apatite-nepheline ores", *Pollution Research, 34*(4). 2015. pp. 809-811.
28. V. B. Kuskov, Ya. V. Kuskova, "Development of technology for the production of natural red iron oxide pigment", *Inzynieria Mineralna (Mineral Engineering), 1*(39). 2017. pp. 217-220.
29. Y. S. Touloukian, C. Y. Ho, "Part II: Thermophysical Properties of Seven Materials*", Thermophysical Properties of Selected Aerospace Materials*. 1976. pp.39-46.
30. J. Lu, E. S. Choi, H. D. Zhou, "Physical properties of Hastelloy C-276 at cryogenic temperatures", *Journal of Applied Physics, 103*. 2008. DOI: 10.1063/1.2899058
31. M. Lanczont, "Numerical Modeling of Superconducting Devices in OpenModelica*", International Conference on Electromagnetic Devices and Processes in Environment Protection with Seminar Applications of Superconductors (ELMECO & AoS)*. 2017. DOI: 10.1109/ELMECO.2017.8267761
32. K. Okuyama, Y. Iida, "Transient boiling heat transfer characteristics of nitrogen (bubble behavior and heat transfer rate at stepwise heat generation*)", International Journal of Heat and Mass Transfer, 33*(10). 1990. pp. 2065 – 2071. DOI: 10.1016/0017-9310(90)90109-8
33. V. Drach, J. Fricke, "Transient heat transfer from smooth surfaces into liquid nitrogen", *Cryogenics, 36*(4). 1996. pp. 263-269. DOI: 10.1016/0011-2275(96)88785-6
34. A. Sakurai, M. Shiotsu, K. Hata, K. Fukuda, "Photographic study on transitions from non-boiling and nucleate boiling regime to film boiling due to increasing heat inputs in liquid nitrogen and water", *Nuclear Engineering and Design, 200*(1-2). 2000. pp. 39-54. DOI: 10.1016/S0029-5493(99)00325-8
35. V. S. Talismanov, S. V. Popkov, O. G. Karmanova, S. S. Zykova, "Synthesis and fungicidal activity of substituted 1-[(1,3-dioxolan-4-yl)]methyl-1H-imidazoles and 1-[(1,3-dioxolan-4-yl)methyl]-1H-1,2,4-triazoles based on arylidene ketones‖, *International Journal of Pharmaceutical Research,11*(2). 2019. pp. 315-319. DOI: 10.31838/ijpr/2019.11.02.051
36. A. Strizhenok, D. Korelskiy, "Assessment of the state of soil-vegetation complexes exposed to powder-gas emissions of nonferrous metallurgy enterprises", *Journal of Ecological Engineering, 17*(4). 2016. pp. 25-29. DOI: 10.12911/22998993/64562
37. V. B. Kuskov, Ya. V. Kuskova, "Research of physical and mechanical properties of briquettes, concentrated from loose high-grade iron ores", *17th International multidisciplinary scientific geoconference SGEM 2017, 17*. 2017. pp. 1011-1015.